Available online at www.sciencedirect.com

ScienceDirect

Nuclear Physics A 932 (2014) 365–372

NUCLEAR PHYSICS A

www.elsevier.com/locate/nuclphysa

Azimuthal correlations with ALICE

A. Dobrin for the ALICE Collaboration

Utrecht University, Princetonplein 5, 3584 CC Utrecht, The Netherlands

Received 2 April 2014; received in revised form 18 July 2014; accepted 20 July 2014

Available online 19 August 2014

Abstract

Measurements of two- and multi-particle azimuthal correlations provide valuable information on the properties of the system created in collisions of hadrons and nuclei at high energy. In this article, the latest results for inclusive and identified charged particle correlations are reported in Pb–Pb, p–Pb and pp collisions recorded by the ALICE detector.

Keywords: ALICE; Azimuthal correlations; Anisotropic flow; Ridge; Uncorrelated seeds

1. Introduction

Azimuthal correlations have become an important observable for the characterization of the properties and the evolution of the system created in a nucleus–nucleus collision [1]. Azimuthal anisotropies in particle production relative to the collision symmetry plane, often referred to as anisotropic flow, have showed that the matter created in heavy–ion collisions behaves as a nearly perfect fluid with low shear viscosity (η/s). In addition, the flow of identified particles allows to probe the freeze-out conditions of the system (e.g. radial flow) as well as the hadronization mechanism.

Anisotropic flow arises due to the asymmetry in the initial geometry of the collision. It is expected to reflect the shape and fluctuations in the initial energy density of the collision [1]. The magnitude of the anisotropic flow is characterized by the Fourier coefficients [2,3]:

$$v_n(p_{\mathrm{T}}, \eta) = \left\langle \cos\left[n(\phi - \Psi_{\mathrm{n}})\right] \right\rangle, \tag{1}$$

E-mail address: alexandru.florin.dobrin@cern.ch (A. Dobrin).

http://dx.doi.org/10.1016/j.nuclphysa.2014.07.029

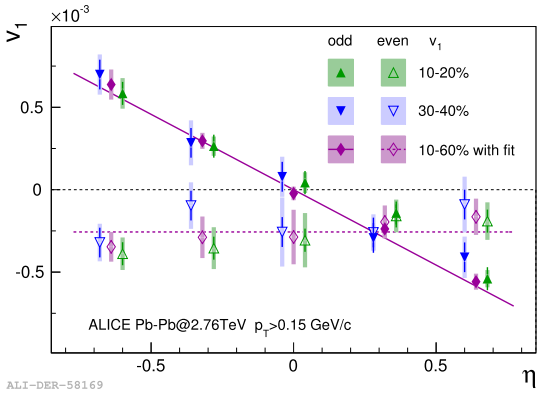

Fig. 1. (Color online.) v_1^{odd} and v_1^{even} as a function of pseudorapidity for various centrality classes in Pb–Pb collisions [8]. Lines represent linear fits for v_1^{odd} and v_1^{even} for the 10–60% centrality class.

where p_T, η, and ϕ are the particle's transverse momentum, pseudorapidity, and the azimuthal angle, respectively, and Ψ_n is the n-th harmonic symmetry plane angle. The flow coefficients v_n are measured using various methods which have different sensitivity to flow fluctuations and correlations unrelated to the azimuthal asymmetry in the initial geometry ("non-flow"). For a smooth matter distribution in the colliding nuclei, all odd Fourier coefficients are zero by symmetry. The fluctuations in the initial geometry contribute to the difference in flow coefficients calculated from two- or multi-particle azimuthal correlations and give rise to non-zero odd harmonic coefficients. The second and the third Fourier coefficients are called elliptic and triangular flow, respectively.

Large elliptic flow (v_2) and significant triangular flow (v_3) of inclusive and identified charged particles were observed at the Large Hadron Collider [4–6]. In this article we review the latest results on inclusive and identified charged particle azimuthal correlations in Pb–Pb, p–Pb and pp collisions at $\sqrt{s_{NN}} = 2.76$ TeV, $\sqrt{s_{NN}} = 5.02$ TeV and $\sqrt{s} = 7$ TeV, respectively, recorded by the ALICE detector [7].

2. Results

The charged particle v_1 has been measured relative to the deflection of spectator neutrons using the Zero Degree Calorimeters [7]. Fig. 1 presents the v_1^{even} and v_1^{odd} components as a function of pseudorapidity for different centrality classes [8]. The v_1^{odd} component exhibits a negative slope with a weak centrality dependence and a magnitude about three times smaller than at top RHIC energy [9]. The v_1^{even} component is negative and independent of pseudorapidity and centrality within uncertainties, consistent with dipole-like fluctuations of the initial energy density of the collision.

Measurements of v_2 and v_3 flow coefficients over a large pseudorapidity range ($|\eta| < 5$) [11] have been performed with two-particle cumulant method [10] using charged particle hits in the Forward Multiplicity Detector [7] and clusters from the first layer of the Silicon Pixel Detector [7] (see Fig. 2). The η-differential v_2 has a strong centrality dependence, while v_3 shows little centrality dependence with a magnitude significantly smaller than that of v_2.

The relative difference between elliptic flow results obtained from two- and four-particle cumulant methods, $[(v_2\{2\}^2 - v_2\{4\}^2)/(v_2\{2\}^2 + v_2\{4\}^2)]^{1/2}$, allows one to study flow fluctuations

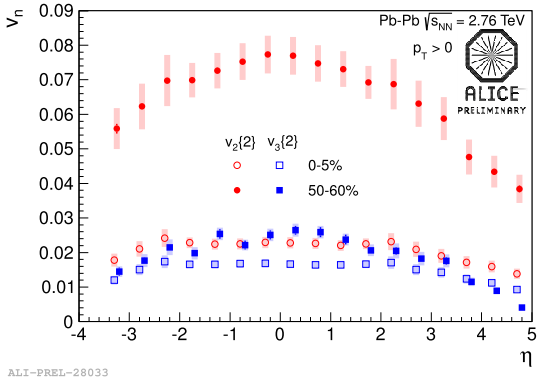

Fig. 2. (Color online.) v_2 and v_3 as a function of pseudorapidity for various centrality classes in Pb–Pb collisions [11].

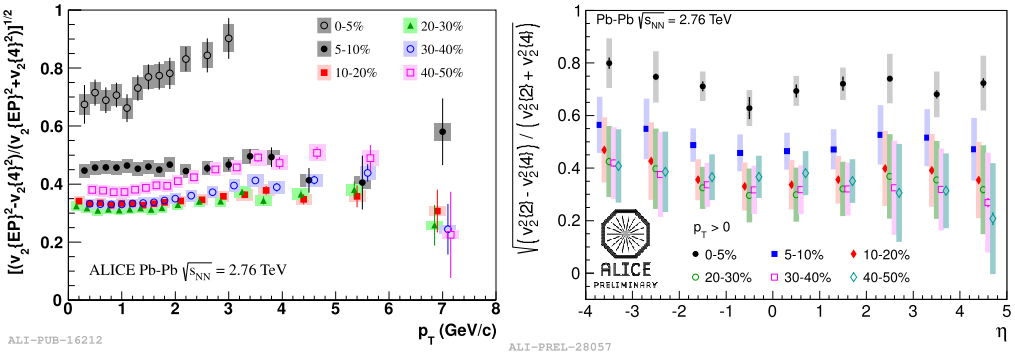

Fig. 3. (Color online.) Relative flow fluctuations (see text for definition) as a function of transverse momentum (left) [6] and pseudorapidity (right) [11] for various centrality classes in Pb–Pb collisions.

at large transverse momenta and forward pseudorapidity regions. For small non-flow contributions this difference is proportional to the relative flow fluctuations, $\sigma_{v_2}/\langle v_2 \rangle$ [1]. Fig. 3 presents this quantity as a function of transverse momentum (left) and pseudorapidity (right) for different centrality classes. The relative flow fluctuations, usually associated with fluctuations in the initial geometry, are almost independent on pseudorapidity and momentum within uncertainties (except 0–5% and 40–50% centrality classes). This suggests a common origin of flow fluctuations up to $p_T = 8$ GeV/c and $|\eta| < 5$. A strong centrality dependence is found for both measurements.

The nature of flow fluctuations can also be investigated by studying the inter-correlation among different symmetry planes [12]. Fig. 4 presents the 3-particle correlator $\langle \cos(\phi_a - 3\phi_b + 2\Psi_2) \rangle$ as a function of transverse momentum of the first particle a for various centrality classes [13]. It probes the correlation between the first, second and third harmonic symmetry planes and has been proposed in [14]. The results agree qualitatively with ideal hydrodynamic model calculations with Glauber initial conditions [14] for $p_T < 2$ GeV/c, while they differ significantly from predictions at higher p_T. The centrality dependence of the 5-particle cumulant results is shown in Fig. 5 [13]. The correlation between the second and third $(v_3^2 v_2^3 \cos[6(\Psi_3 - \Psi_2)])$, the first and second $(-v_2^3 v_1^2 \cos[2(\Psi_2 - \Psi_1)])$, the first, second and third $(-v_3 v_2^3 v_1 \cos[3\Psi_3 - 2\Psi_2 - \Psi_1])$ symmetry planes is depicted by the green, red and blue markers,

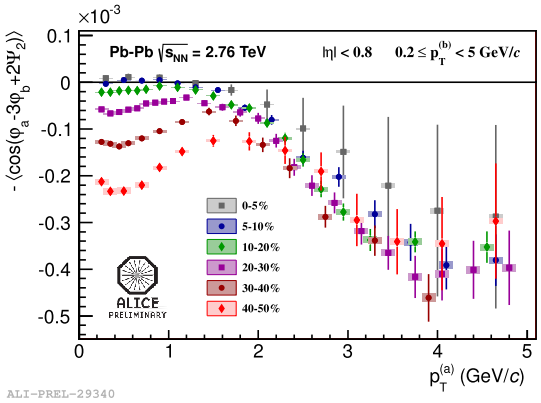

Fig. 4. (Color online.) 3-particle correlator as a function of transverse momentum for various centrality classes in Pb–Pb collisions [13].

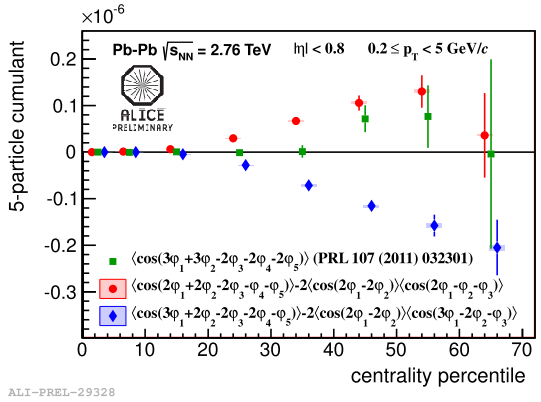

Fig. 5. (Color online.) 5-particle cumulants as a function of centrality in Pb–Pb collisions [13].

respectively. The results of 3- and 5-particle correlations indicate the existence of three plane correlations between Ψ_1, Ψ_2 and Ψ_3 in mid-central collisions, while the correlation between Ψ_2 and Ψ_3 is negligible for the same centrality classes.

Identified particle anisotropic flow adds further constraints to initial conditions, transport coefficients (η/s), freeze-out parameters (temperature, radial flow), particle production mechanism (hydrodynamics, coalescence, fragmentation of high energy partons). At low transverse momenta, $p_{\mathrm{T}} < 2$–3 GeV/c, the flow pattern is qualitatively described by hydrodynamic model calculations which exhibit typical mass dependence [15]. For $3 < p_{\mathrm{T}} < 8$ GeV/c, the flow of baryons is larger than that of the mesons [6] which may be attributed to quark coalescence [16]. At large transverse momenta, $p_{\mathrm{T}} > 8$ GeV/c, anisotropic flow is believed to reflect the path length dependence of the parton energy loss [17].

Fig. 6 presents the v_2 coefficients for charged π, K, $\bar{\mathrm{p}}$, $\mathrm{K}^0_{\mathrm{S}}$, Λ as a function of transverse momentum for the 10–20% centrality class in Pb–Pb collisions [18] together with viscous hydrodynamic calculations using Color Glass Condensate (CGC) initial conditions with $\eta/s = 0.2$ [19]. The results were obtained with the scalar product method [1] using a large η gap ($|\Delta\eta| > 1$) between particle of interest (POI) and reference particles (RPs) in order to suppress non-flow.

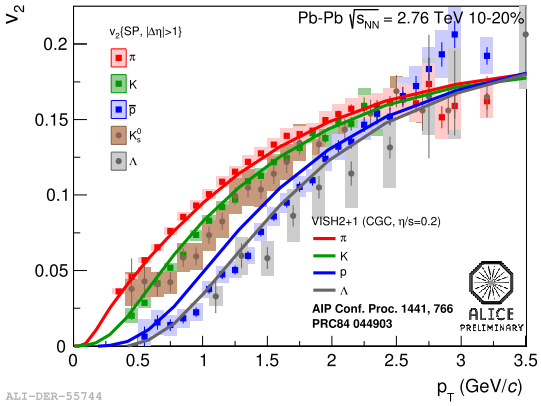

Fig. 6. (Color online.) The v_2 coefficients for identified particles as a function of transverse momentum for the 10–20% centrality class in Pb–Pb collisions [18]. The solid lines represent viscous hydrodynamic calculations [19].

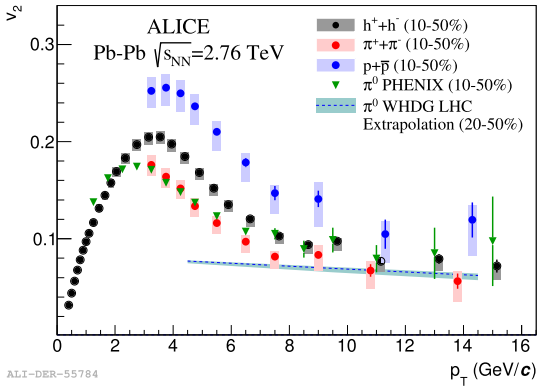

Fig. 7. (Color online.) The v_2 coefficients for unidentified charged particles, pions and (anti-)protons as a function of transverse momentum for the 10–50% centrality class in Pb–Pb collisions [6]. The v_2 for pions is compared with PHENIX π^0 v_2 measurements [21] and WHDG model calculations for neutral pions [20] extrapolated to the LHC collision energy.

A clear mass splitting is found for $p_T \leq 2$ GeV/c attributed to the interplay between elliptic and radial flow. The model reproduces the main features of v_2 for pions and kaons up to $p_T \sim 2$ GeV/c, but overestimates v_2 for $\bar{p}$ and Λ. A better agreement is found in peripheral collisions [18]. The v_2 for protons crosses the one of charged pions at $p_T \approx 2$ GeV/c and has a larger magnitude up to $p_T = 8$ GeV/c, indicating that particle type dependence extends to intermediate/high p_T (see Fig. 7). The flow coefficients presented in Fig. 7 are measured using the event plane method [1] with a pseudorapidity gap of $|\Delta\eta| > 2$ between POI and particles used to estimate the event plane angle [6]. The v_2 for charged pions is reproduced by WHDG calculations of neutral pions [20] for $p_T > 8$ GeV/c and is similar in magnitude to that measured at RHIC [21] out to $p_T = 16$ GeV/c.

An analysis based on two-particle correlations technique has also been performed in p–Pb collisions at $\sqrt{s_{NN}} = 5.02$ TeV [22]. It was done by measuring particle pairs from same events as a function of relative pair angles $\Delta\phi$ and $\Delta\eta$. The results were corrected for pair acceptance

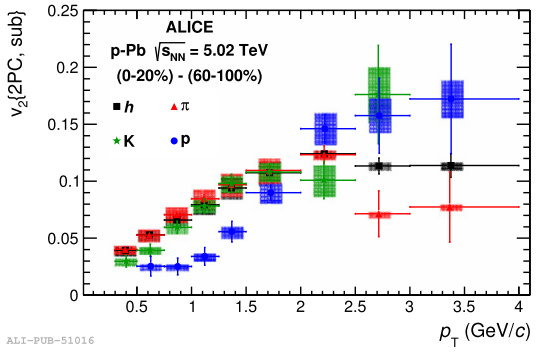

Fig. 8. (Color online.) The v_2 coefficients for inclusive and identified charged particles as a function of transverse momentum for the 0–20% multiplicity class after applying the subtraction procedure (see text) in p–Pb collisions [22].

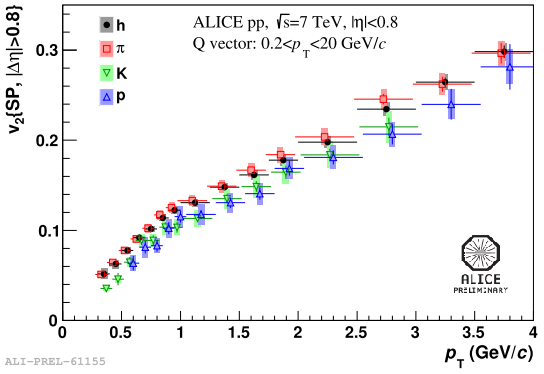

Fig. 9. (Color online.) The v_2 coefficients for inclusive and identified charged particles as a function of transverse momentum in minimum bias pp collisions.

and efficiency using mixed events. Only unidentified charged particles were used as trigger particles, while for associated particles unidentified and identified charged particles were selected (denoted as h–h, h–π, h–K, h–p correlations). The two-particle correlations were studied in four event classes defined as fractions of the analyzed event sample and denoted "0–20%", "20–40%", "40–60%", "60–100%" from the highest to lowest multiplicity. In order to remove the jet contributions, the associated yield per trigger particle in $\Delta\phi$ and $\Delta\eta$ from low multiplicity (60–100%) events was subtracted from the corresponding yield of 0–20% multiplicity class. More details about the subtraction method can be found in [23]. This procedure revealed a double-ridge structure for h–h, h–π, h–K, h–p correlations. The residual near side jet contribution is further suppressed by applying a $|\Delta\eta| > 0.8$ gap. The per-trigger yield was projected onto $\Delta\phi$ and was fitted with a Fourier series. Fig. 8 presents v_2 coefficients for h, π, K, p. A mass ordering is observed between pions and protons for $p_T < 2$ GeV/c ($v_2^p < v_2^\pi$), while $v_2^p > v_2^\pi$ for $p_T > 2.5$ GeV/c; the crossing happens at $p_T \approx 2$ GeV/c. For $p_T < 1$ GeV/c, there is a hint that kaons follow this ordering. The observed mass ordering and the crossing between proton and pion v_2 is qualitatively similar to observations in Pb–Pb collisions (see Fig. 6).

Fig. 9 shows v_2 coefficients for inclusive and identified charged particles as a function of momentum in minimum bias pp collisions at $\sqrt{s} = 7$ TeV. The scalar product method with a

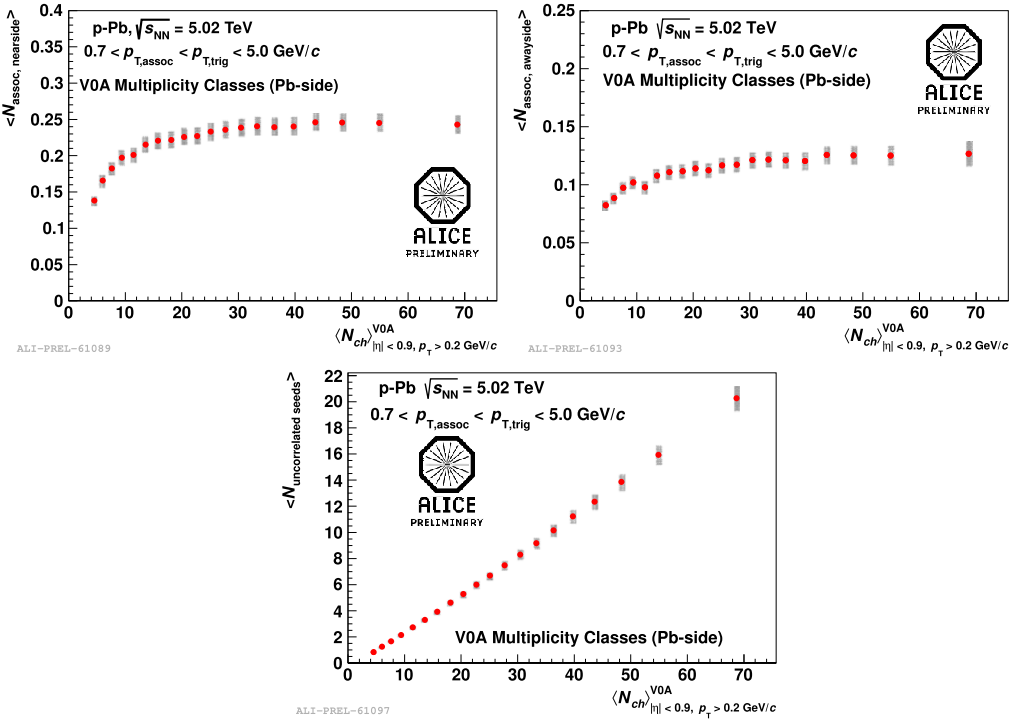

Fig. 10. (Color online.) Near side yield (top left), away side yield (top right) and uncorrelated seeds (bottom) as a function of multiplicity at midrapidity for different event classes in p–Pb collisions [24].

$|\Delta\eta| > 0.8$ gap between POI and RPs was used in the analysis in order to suppress the dominating non-flow contributions. The coefficient v_2^{p} is lower than v_2^{π} over the entire p_{T} range, while the coefficient v_2^{K} is consistent with v_2^{p} for $p_{\mathrm{T}} < 3$ GeV/c. The observed behavior is different than that in Pb–Pb and p–Pb collisions.

Another analysis based on two-particle correlations was performed to measure the number of multiple parton interactions (MPIs) in p–Pb collisions [24]. As before, the correlation between trigger and associated particles (both unidentified charged hadrons) was measured as a function of the angular differences $\Delta\phi$ and $\Delta\eta$. The same correction procedure from mixed events was also used here. A double ridge subtraction was done in order to suppress the non-jet related components (for details see [24]). The near and away side yields were extracted using zero yield at minimum (ZYAM) bin counting method. Fig. 10 presents the near side yield (top left), away side yield (top right) and uncorrelated seeds (bottom) as a function of multiplicity for different event classes in p–Pb collisions. The near and away side yields show an increase from low to intermediate multiplicity and flatten for high multiplicities. These observations indicate that high multiplicity p–Pb collisions are not characterized by a higher number of associated particles in the jet peaks. Both yields increase with multiplicity in pp collisions [25]. The uncorrelated seeds (number of independent sources of particle production) are calculated according to

$$N_{\text{uncorrelated seeds}} = \frac{\langle N_{\text{trig}} \rangle}{\langle 1 + N_{\text{assoc, NS}} + N_{\text{assoc, AS}} \rangle}, \tag{2}$$

where N_{trig}, $N_{\mathrm{assoc,\,NS}}$ and $N_{\mathrm{assoc,\,AS}}$ are the number of trigger particles, near side and away side associated yields per trigger particle, respectively. A strong correlation between uncorrelated seeds and MPIs is found in PYTHIA, regardless of the η range [25]. The MPIs increase with multiplicity in p–Pb collisions, while the number of uncorrelated seeds saturate in pp collisions [25].

3. Summary

The extended ALICE flow measurements allow for unprecedented study of the system created in Pb–Pb collisions. We have found that flow fluctuations are similar for $|\eta| < 5$ and up to $p_{\mathrm{T}} = 8$ GeV/c, except for very central collisions. The identified particle flow shows a clear mass splitting at low transverse momenta and is well described by hydrodynamic model calculations. For $3 < p_{\mathrm{T}} < 8$ GeV/c, the (anti-)proton v_2 is higher than that of pions indicating that particle type dependence persists out to high p_{T}. These results point out that jet quenching completely dominates the particle production mechanism for $p_{\mathrm{T}} > 8$ GeV/c, while hydrodynamics plays the main role for $p_{\mathrm{T}} < 2$ GeV/c. Different scenarios are available for the intermediate p_{T} region which is less understood. Recent azimuthal correlation studies in p–Pb collisions yielded rather intriguing similarities to the Pb–Pb measurements. The observed behavior of identified particle v_2 in pp collisions differs from the one seen in Pb–Pb and p–Pb collisions.

References

[1] S.A. Voloshin, A.M. Poskanzer, R. Snellings, in: Relativistic Heavy Ion Physics, in: Landolt–Boernstein, vol. 1/23, Springer-Verlag, 2010, pp. 5–54.
[2] S. Voloshin, Y. Zhang, Z. Phys. C 70 (1996) 665.
[3] A.M. Poskanzer, S.A. Voloshin, Phys. Rev. C 58 (1998) 1671.
[4] K. Aamodt, et al., ALICE Collaboration, Phys. Rev. Lett. 105 (2010) 252302.
[5] K. Aamodt, et al., ALICE Collaboration, Phys. Rev. Lett. 107 (2011) 032301.
[6] B. Abelev, et al., ALICE Collaboration, Phys. Lett. B 719 (2013) 18.
[7] K. Aamodt, et al., ALICE Collaboration, J. Instrum. 3 (2008) S08002.
[8] B. Abelev, et al., ALICE Collaboration, Phys. Rev. Lett. 111 (2013) 232302.
[9] B.I. Abelev, et al., STAR Collaboration, Phys. Rev. Lett. 101 (2008) 252301.
[10] A. Bilandzic, R. Snellings, S. Voloshin, Phys. Rev. C 83 (2011) 044913.
[11] A. Hansen, ALICE Collaboration, Nucl. Phys. A 904–905 (2013) 523c.
[12] R.S. Bhalerao, M. Luzum, J.-Y. Ollitrault, Phys. Rev. C 84 (2011) 054901.
[13] A. Bilandzic, ALICE Collaboration, Nucl. Phys. A 904–905 (2013) 515c.
[14] D. Teaney, L. Yan, Phys. Rev. C 83 (2011) 064904.
[15] P. Huovinen, P.F. Kolb, U.W. Heinz, P.V. Ruuskanen, S.A. Voloshin, Phys. Lett. B 503 (2001) 58.
[16] D. Molnar, S.A. Voloshin, Phys. Rev. Lett. 91 (2003) 092301.
[17] R.J.M. Snellings, A.M. Poskanzer, S.A. Voloshin, arXiv:nucl-ex/9904003.
[18] F. Noferini, ALICE Collaboration, Nucl. Phys. A 904–905 (2013) 483c.
[19] U. Heinz, C. Shen, H. Song, AIP Conf. Proc. 1441 (2012) 766.
[20] W.A. Horowitz, M. Gyulassy, J. Phys. G 38 (2011) 124114.
[21] A. Adare, et al., PHENIX Collaboration, Phys. Rev. Lett. 105 (2010) 142301.
[22] B. Abelev, et al., ALICE Collaboration, Phys. Lett. B 726 (2013) 164.
[23] B. Abelev, et al., ALICE Collaboration, Phys. Lett. B 719 (2013) 29.
[24] E. Leogrande, ALICE Collaboration, Nucl. Phys. A 932 (2014) 409–414, in this issue.
[25] B. Abelev, et al., ALICE Collaboration, J. High Energy Phys. 1309 (2013) 049.